Int J Civ Eng (2018) 16:629–646
https://doi.org/10.1007/s40999-016-0138-7

RESEARCH PAPER

Effect of Timber Type and Nail Spacing on the Hysteretic Behavior of Timber-Framed Shear Walls with Openings

Özgür Anil[1] · Abdullah Togay[2] · Ümmü Karagöz Işleyen[3] · Nihat Döngel[4] · Cevdet Söğütlü[4]

Received: 17 August 2016 / Revised: 10 December 2016 / Accepted: 15 December 2016 / Published online: 17 February 2017

Abstract In scope of the study, behavior of timber-framed shear walls having openings with variable dimensions and locations subjected to reverse cyclic loading is experimentally investigated. Main variables considered in the study are the aspect ratios of timber-framed panel walls, dimensions and locations of the openings on the panel walls, material of the timber frames and spacings of the nails used in the panel connections. Load–displacement relationships, strengths, stiffnesses, displacement ductility ratios, energy dissipation capacities and failure mechanisms of the specimens are determined. The ultimate load capacities of the timber-framed panels are calculated as per Eurocode 5 and presented in comparison to experimental results. Moreover, lateral load-resisting capacities and load–displacement relationships of the test specimens are numerically calculated with finite element analyses. A good agreement was observed between the numerical and experimental results. From the test results, it is observed that the load behavior relationships of the test specimens significantly affected by aspect ratios, location of the openings, material of the timber frames and spacing of the nails used to provide connection between the timber-framed panel elements. Also, the increasing size of the openings decreased the stiffness' of the test specimens.

Keywords Timber-framed shear wall · Hysteretic behavior · Finite element analysis · Cyclic load · Opening

✉ Özgür Anil
oanil@gazi.edu.tr

[1] Engineering Faculty, Civil Engineering Department, Gazi University, Ankara, Turkey

[2] Architecture Faculty, Department of Industrial Design, Gazi University, Ankara, Turkey

[3] Faculty of Forestry, Dept. of Wood Products Industrial Engineering, Kastamonu University, Kastamonu, Turkey

[4] Faculty of Technology, Department of Wood Products Industrial Engineering, Gazi University, Ankara, Turkey

Abbreviations

Conversion factors

1 mm	0.039 in
1 mm^2	0.00152 in^2
1 kN	0.2248 kips
1 MPa	145 psi

Symbols

$F_{v,\mathrm{Rd}}$	Design racking load-carrying capacity of wall
$F_{f,\mathrm{Rd}}$	Lateral design capacity of an individual fastener
B	Wall panel width
s	Fastener spacing
h	Height of the wall
d	Fastener diameter (m)
ρk	Density of the timber frame (kg/m^3)
s_0	Basic fastener spacing (see Eq. 4)
k_d	Dimension factor for the panel
k_{iq}	Uniformly distributed load factor for wall i
k_s	Fastener spacing factor
k_n	Sheathing material factor
K_ser	Slip modulus of a connection for the serviceability limit state (N/mm)
K_u	Slip modulus of a connection for the ultimate limit state (ULS) (N/mm)
ρ_m	Mean densities $\rho_{m,1}$ and $\rho_{m,2}$ (kg/m^3)
$\rho_{m,1}$	Density of wood frame (spruce, fir, pine)
$\rho_{m,2}$	Density of sheathing panel (OSB, 590 kg/m^3)
d	Fastener diameter (mm) (in Eq. 5)

1 Introduction

Timber structures have been commonly used in the earthquake-prone countries since many years. However, in the literature, in contrast to the fact that there are plenty of studies considering the behavior of reinforced concrete, masonry and steel structures, there are a limited number of comprehensive studies focused on the behavior of timber structures subjected to ground motion excitations [1].

The main resistance, stiffness and energy dissipation capacities of the timber structures under lateral loads are provided by timber-framed panel walls. Timber structures are constructed by combining the timber-framed panel walls in relation to architectural concerns [2]. The timber-framed panel walls are structural elements similar to the shear walls in reinforced concrete structures or bearing walls in the masonry structures [3]. They significantly contribute to the strength, stiffness and energy dissipation capacities of the timber structures [3]. To investigate the behavior of timber structures under ground motion excitations, an experimental study focused on the behavior of timber-framed panel walls under earthquake-induced lateral loads was planned. Timber-framed panel walls are constructed using timber frame elements and OSB plates, composed of pressed timber particles, used to cover the surface of the wall [2, 3]. Connection, with connector links, of these timber frame elements and OSB plates forms the load-carrying panel walls. The major advantages of timber structures compared to traditional buildings are sound physical properties, reduced power consumption, construction speed and factory production of prefabricated elements. All building elements and details are carefully designed and precisely manufactured in accordance with work plans, which allow contacts to align perfectly [4]. According to Thelandersson and Larsen [2], experiences from earthquake-prone areas indicate that timber structures generally exhibit good seismic performance. Their advantages lie mainly in the low weight of the structure, ductile joints and regularity of the structure. Timber structures represent a significant part of the construction industry in many countries around the world. One of the commonly used solutions for both single- and multi-story buildings is the prefabricated timber structures with timber-framed wall elements as the main vertical load-bearing members. In general, the load-bearing capacity of the timber frame resists most of the vertical loads, while the sheathing boards provide the horizontal stability, i.e., their main function is resisting horizontal (wind and seismic) loads. Using adequate shear connection between the components, the wall elements may be considered as composite systems taking advantage of the favorable properties of both materials [5].

Increasing number of timber structures also increased the number of studies conducted focused on the timber structures. The parameters that affect the behavior and performance of timber-framed panel walls have been experimentally investigated in the research studies [6–10]. In such studies, generally the tests were conducted on the timber-framed panels with unit dimensions used in the construction of timber structures. Moreover, in addition to experimental studies, analytical and numerical studies were conducted to calculate the lateral load-resisting capacities of the timber-framed panel walls [11, 12]. In conventional buildings (i.e., residential, office, etc.), a significant part of the wall elements may have one or more openings for functional reasons, such as doors or windows. The openings reduce the stiffness of the structure. Also additional problems may arise due to stress concentrations at the corners. Several research studies have been published in the past discussing the influence of the openings on the load-bearing capacity of different structures, e.g., reinforced concrete shear walls [13, 14], and plywood-sheathed timber frame wall elements [15, 16]. In the international literature, it was observed that there were a limited number of studies on this subject [6–8, 17]. From the literature review, it is observed that conducted experimental and analytical studies generally focused on the typical timber-framed panel walls with standard geometries. From these studies, it is also observed that the test specimens were tested under lateral monotonic loading conditions. For such reasons, a comprehensive experimental study including test specimens constructed from different materials as combinations of timber-framed panel walls with different aspect ratios and, openings with variable dimensions and locations. In the study, these test specimens are subjected to reverse cyclic repeated loading.

In addition, experimentally verified finite element models of the timber-framed panels are constructed in this study. In recent years, numerical research studies based on the 2D and 3D finite element models were conducted [18–20]. These studies were focused on the behavior of connector elements used to connect element forming timber-framed shear panels. The load–displacement relationships of the connector elements were obtained from the conducted experimental studies [21]. Based on these, hysteretic material models are proposed to model the cyclic behavior of connector elements. Then, it was observed that these models were successful in the modeling of general cyclic behavior of timber-framed shear panels [22].

Also, there are several numerical studies that attempted to model the nonlinear behavior of timber-framed shear walls. Gupta and Kuo [23] developed a model for wood-frame buildings made up of seven super-elements, and having nine global degrees of freedom. Ayoub [24] proposed energy-based hysteretic models to simulate the

nonlinear earthquake response of timber structures. In the proposed model, different types of damage occurring in the experiments of timber structures are simulated. Guan ve Zhu [25] used the Tsai Hill yield criterion to simulate the anisotropic plastic behavior of OSB and timber. In the analyses, the software ABAQUS was used to simulate the behavior of I beams which are modeled as anisotropic elastic plastic composite beams. In the finite element studies, generally beam elements for frame members, shell elements for OSB panels and springs for connector elements are used [24, 26–28]. Furthermore, diagonal strut approach is used to simulate the behavior of timber panels and to develop the mathematical models [4].

Main variables considered in the experimental study are the aspect ratios of timber-framed panel walls, dimensions and locations of the openings on the panel walls, material of the timber frames and spacings of the nails used in the panel connections. In scope of the experimental study, 13 test specimens were manufactured and tested under ground motion simulating reverse cyclic repeated loading. From the experimental study, load–displacement relationships, strengths, stiffnesses, displacement ductility ratios, energy dissipation capacities and failure mechanisms of the specimens are determined. Results from the experimental study were compared with the analytical results calculated using Eurocode 5 [29] in terms of load-resisting capacities. Furthermore, the finite element software ANSYS was used to perform finite element analyses of test specimens and numerical results were comparatively presented.

2 Experimental Program

2.1 Test Specimens and Material

In scope of the experimental study behavior of timber-framed shear walls, the main load-resisting elements in the timber structures are investigated under reverse cyclic loading conditions. In the study, 13 timber-framed test specimens were manufactured and tested. Test specimens were manufactured with typical geometrical dimensions without any scaling procedure. Variables considered in the study are the aspect ratios of timber-framed panel walls, dimensions and locations of the openings on the panel walls, material of the timber frames and spacings of the nails used in the panel connections. Properties of the test specimens are presented in Table 1. From the table, it is observed that aspect ratios of the test specimens were 0.45, 0.68 and 1.13. These aspect ratios were selected to observe the effects of aspect ratio on the general load–displacement behavior and failure mechanisms. Another variable considered in the study was the material type used in the manufacturing of timber frames. In scope of the study, three common timber types (spruce tree, fir tree, pine) were used in the manufacturing of timber-framed panel walls. The opening dimensions of the panel walls were other variables considered in the study. The specimens have one or more openings with variable dimensions and locations. From the test specimens 12 and 13, effect of the spacings of the nails used in the connection of the OSB panels and timber frame elements was considered.

Timber-framed panel walls were manufactured using two main structural elements. These structural elements were timber frames and OSB plates used to cover the surface of the frame. The production of test specimens was started by bringing together the pieces of timber frame material in a manner that would form a frame in the dimensions of 38 × 140 mm. In the joining of the frame elements 2, each No. 10, wood screws (5 × 100 mm) were used for the lower and upper horizontal pieces and 2, each No. 10, wood screws were used in the joining of the vertical side and central pieces, whereas, nails (3.1 × 80 mm) were used in the joining of the OSB surface sheathing material with the timber frame elements. A pneumatic nail driving machine was used in the nail driving process.

Production of timber frames was completed using OSB sheathing materials with a standard thickness of 11 mm. The OSB and the timber frame were connected to each other using nails. The nails were placed at 100 mm intervals on the external edges of the timber frame and at 300 mm intervals on the perpendicular and horizontal elements of the central section except the specimen 13. The nails with 300 mm spacing were used in the connection of timber frame elements with the inner and outer sides of the OSB plates. The elements and components, which formed the standard timber-framed shear wall, have been shown in Fig. 1. Heat insulation materials were not placed on the test specimens in the experimental program. The dimensions of the test specimens are given in Fig. 2. Some photographs of the test specimens in the manufacturing procedure are given in Fig. 3. The material properties used in the manufacturing of the test specimens and finite element analyses are given in Table 2. Spruce tree, fir tree and pine were used in the manufacturing of test specimens. The mechanical properties of the test specimens are determined through tests as per different codes.

Density of the timber was determined through tests as per TS2472, 1976 [30], bending modulus of elasticity was determined through tests as per TS2478, 1976 [31], tension strength parallel to fibers was determined through tests as per TS2475, 1976 [32], and compression strength parallel to fibers was determined through tests as per TS2595, 1977 [33] Measurements presented in Table 2 were obtained by performing five tests on specimens. The mechanical properties of OSB plates are also given in Table 2. The

Table 1 Properties of Specimens

Specimen no	Timber wall width/height (mm)	Width/height ratio	Wood type	Nail spacing (mm)	Timber wall configuration
1	3000/2650	1.13	Spruce	100	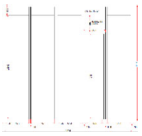
2	3000/2650	1.13	Spruce	100	
3	3000/2650	1.13	Fir	100	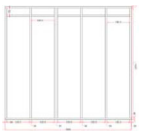
4	3000/2650	1.13	Pine	100	
5	3000/2650	1.13	Spruce	100	
6	3000/2650	1.13	Fir	100	
7	3000/2650	1.13	Pine	100	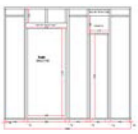
8	3000/2650	1.13	Spruce	100	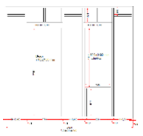
9	1200/2650	0.45	Spruce	100	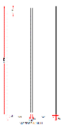
10	1200/2650	0.45	Pine	100	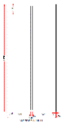
11	1200/2650	0.45	Fir	100	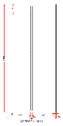
12	1800/2650	0.68	Spruce	100	

Table 1 continued

Specimen no	Timber wall width/height (mm)	Width/height ratio	Wood type	Nail spacing (mm)	Timber wall configuration
13	1800/2650	0.68	Spruce	300	

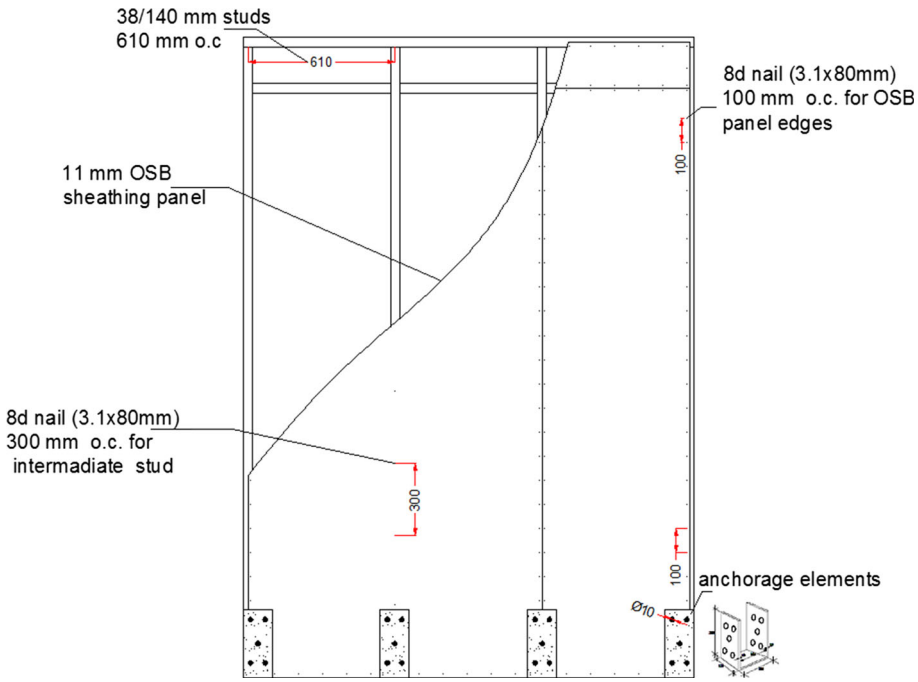

Fig. 1 Schematic of standard timber-framed shear wall

densities of OSB plates were measured according to TS EN323, 1999 [34] and its modulus of elasticity was obtained according to TS EN310, 1999. [35] The tensile and compressive strength of the OSB plates were obtained as per ASTM D 3500-14, 2014 [36] and ASTM D 3501-05a, 2011 [37], respectively. The material properties of the timber screws (5 × 100 mm) and nails (3.1 × 80 mm), used to connect OSB plates and timber frame, are provided by manufacturers. The yield strength of the timber screws is 552 MPa, tensile strength is 400 MPa and modulus of elasticity is 202 GPa. The yield strength of nails (3.1 × 80 mm), used to connect OSB plates and timber frame, is 690 MPa, the tensile strength was 600 MPa and the modulus of elasticity is 210 GPa.

2.2 Experimental Setup

The experiments on the specimens were conducted under the reverse cyclic loading conditions to simulate ground motion excitations. Steel support pieces were used to attach and fix the specimens to the reinforced concrete rigid test platform. Loading was applied with a loading column placed between the reinforced concrete rigid wall and the test specimens. Loading was applied using a 400 kN capacity hydraulic jack and measured with a load cell. A special out-of-plane movement-preventing system was manufactured from steel to keep the test specimens in the plane of the timber-framed shear walls under lateral loading conditions. Sticks with bearings located between the test specimens and the frame eliminated the negative effects of friction. The reverse cyclic loading was applied with 5 kN increment until the lateral load-resisting capacity was reached. The tests were finalized by applying two more loading cycles after the maximum load when a 15% drop was observed in the load values. The electronic deformation measurements of the displacement values occurring in the test specimens were measured and transferred via a data accusing system to a computer and stored for later evaluation. The measurements were taken from the test specimens in terms of the horizontal story displacement value,

Fig. 2 Dimensions of test specimens

Fig. 3 Manufacturing process of test specimens

Table 2 Material properties of spruce, pine, fir and OSB

Material properties	Spruce	Pine	Fir	OSB
Density (kg/m^3)	420	520	410	590
Elastic modulus x direction E_X	11,000	11,760	8500	3500
Elastic modulus y direction E_y	900	1100	1060	1585
Elastic modulus z direction E_Z	500	570	780	130
Shear modulus of xy plane G_{xy}	676	1160	880	500
Shear modulus of yz plane G_{yz}	57	66	88	50
Shear modulus of xz plane G_{xz}	636	680	880	100
Poisson ratio of xy plane v_{xy}	0.37	0.42	0.29	0.184
Poisson ratio of yz plane v_{yz}	0.47	0.68	0.39	0.312
Poisson ratio of xz plane v_{xz}	0.42	0.51	0,45	0.364
Tensile strength (MPa)	36.82	73.01	62	6.77
Compression strength (MPa)	55	49.70	37.4	14.19

rigid body turning and sliding and the shear displacement on the OSB plate. Furthermore, in addition to the displacement measurements, the strain measurements were also taken from the horizontal and perpendicular timber elements. A view of the experimental setup is given in Fig. 4.

In the experimental study, axial load was not considered. In timber structures, axial load is generally stays in a low level in relation to the low rise and light nature of timber structures. Moreover, the presence of many load-bearing walls located at the outer surface of the timber structures leads to reduced axial load levels per panel. In addition, the presence of axial load up to a certain level may have a beneficial effect on the moment resisting capacities of panels subjected to horizontal loading. Due to the stated reasons, to consider the worst scenario, the specimens were tested without any axial load.

3 Experimental Results and Evaluations

3.1 Observed Behavior and Failure Modes

Lateral force displacement envelopes of the test specimens, manufactured from spruce tree, fir tree and pine, are given in Fig. 5. The strength, initial stiffness, displacement ductility and energy dissipation capacity values of the test specimens are obtained from these envelope curves. Furthermore, general load–displacement relationships and failure mechanisms are considered and effects of

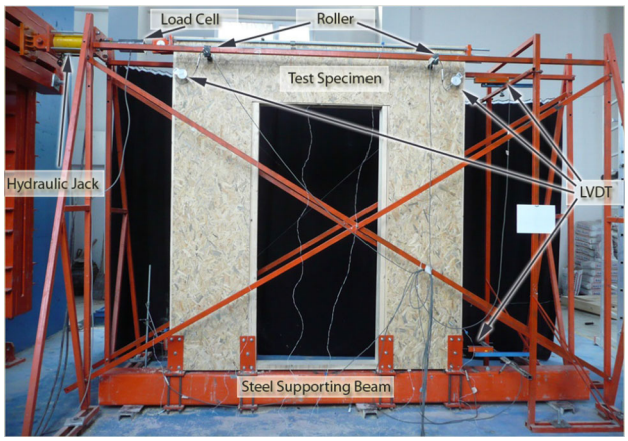

Fig. 4 Test setup and instrumentation

considered variables on these values are investigated. Results obtained from the experiments are given in Table 3. The selected photographs showing the damage on the test specimens are given in Fig. 6.

Decreasing aspect ratio of the test specimens resulted in bending dominated behavior and a large portion of observed displacements was observed as bending displacements.

Increasing aspect ratio values resulted in amplified story displacements due to shear cracks. Measured cracks widths from the specimens with small aspect ratios were observed to be small. The shear crack widths of the test specimens with openings (window or door openings) were amplified due to the shear dominant behavior of the panels.

In the experimental study, considered aspect ratios were 0.45, 0.68 and 1.13. Test specimens with aspect ratio 0.45 (Specimen-9, Specimen-10, Specimen-11) differ from each other in terms of construction materials (i.e., spruce tree, fir tree and pine). Test specimens with aspect ratio 0.68 were Specimen-12 and Specimen-13. Specimen-13 was constructed with nail spacings of 300 mm on the side of OSB plates. Test specimens with aspect ratio 1.13 differ from each other in terms of construction materials and opening ratios. Decreasing aspect ratios decreased the strength and stiffness of the test specimens.

The opening ratio of Specimen-1 was 2%. These ratios were 26% in Specimens-5, 6, 7 and 30% in Specimen-8. From the test results, it was observed that the opening ratios were effective on the variation of maximum strength, stiffness, ductility and energy dissipation capacities. The increasing opening ratios decreased the maximum strength and stiffness values of the test specimens. The specimens with door or window openings react like discrete panels and practically divide the panels into two or three parts. From the comparison of the test specimens separated into discrete panels, it was observed that increasing opening ratio increased the ductility ratio and energy dissipation

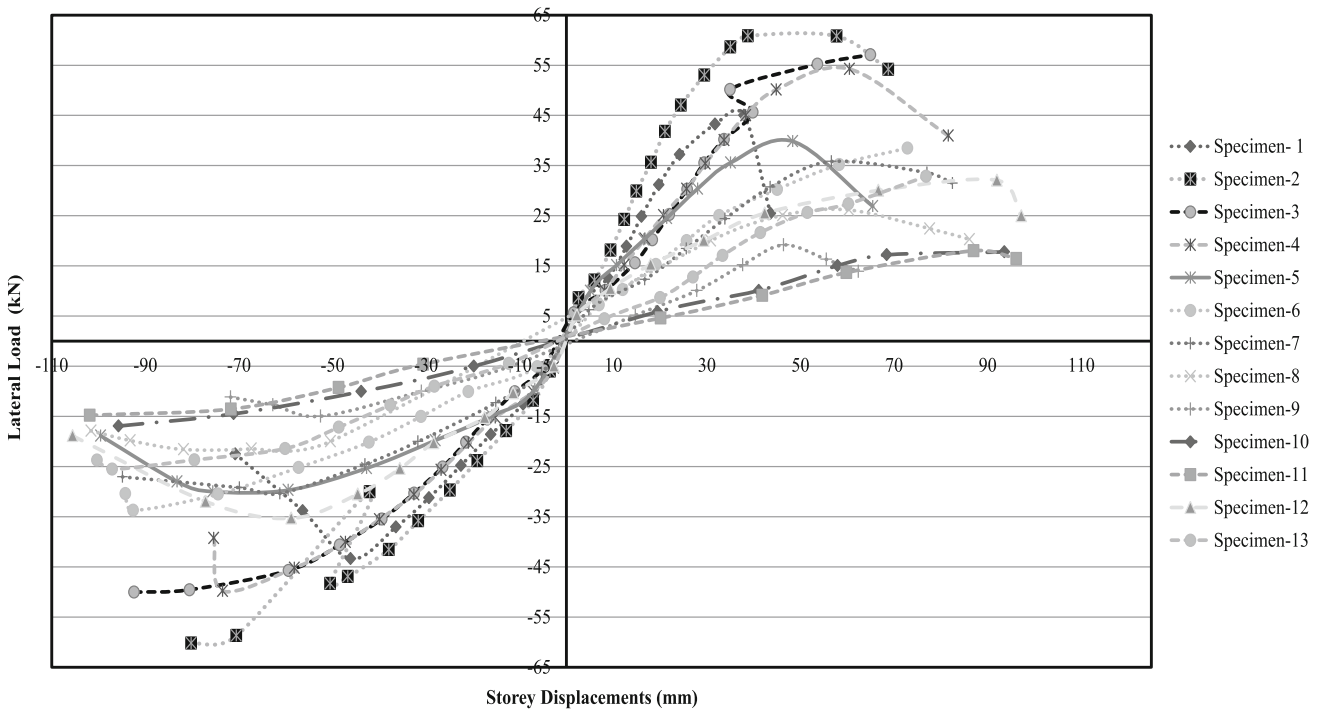

Fig. 5 Envelope curves of load-displacement graphs of specimens

Table 3 Experimental results

Spec. no	Ultimate load (kN)		Displaced at ultimate load (mm)		Initial stiffness (kN/mm)		Ductility ratio	Energy dissipation capacity (kN-mm)	Failure mode
	Forward cycles	Backward cycles	Forward cycles	Backward cycles	Forward cycles	Backward cycles			
1	44.99	−43.40	37.94	−46.12	2.95	1.59	1.18	8507.40	Flexure
2	61.26	−60.24	41.36	−80.22	3.30	1.71	1.66	15,064.49	Flexure
3	57.11	−50.05	64.97	−92.86	3.57	1.07	1.14	14,425.21	Flexure
4	54.24	−49.82	60.51	−73.46	2.10	1.92	1.35	11,727.40	Flexure
5	39.83	−30.40	48.37	−68.03	1.92	1.80	1.46	8106.67	Shear
6	38.49	−33.73	72.90	−92.62	1.04	0.82	1.07	7478.58	Shear
7	35.81	−30.38	56.65	−61.23	1.29	1.19	1.53	7738.24	Shear
8	26.14	−21.60	60.38	−81.80	0.65	0.39	1.98	6499.88	Shear
9	19.16	−14.97	46.53	−52.54	0.42	0.35	1.18	2420.85	Flexure
10	17.78	−16.94	93.97	−95.74	0.30	0.25	1.37	2798.59	Flexure
11	18.03	−14.78	87.03	−101.89	0.23	0.15	1.10	2662.00	Flexure
12	32.06	−35.32	93.04	−58.79	3.19	2.71	1.22	4690.65	Flexure
13	27.53	−25.66	60.25	−96.89	0.55	0.37	1.43	5978.22	Flexure

Fig. 6 Cracking example photos of specimen after test

capacities. Stress concentrations and shear cracks were observed at the corners of the openings in such panels.

Test aspect ratios test specimens 12 and 13 are 0.68. The only difference of these test specimens is the spacing of the nails located at the sides of the OSB panel. On test specimen 13, the nail spacings were 300 mm. From the test results, it was observed that increasing nail spacing (i.e., a smaller number of nails) resulted in lower initial stiffness values leading to amplified displacements under smaller ultimate load levels.

Spruce tree, fir tree and pine are commonly used materials in the construction of timber structures. Generally, these timber types are considered as a group and commonly known as Spruce-pine-fir (SPF). SPF group timbers are commonly used in the construction of timber structures due to their high strength, low weight, good nail confining and workability properties. The performance of the test specimens conducted in this study is investigated to observe the suitability of the spruce tree and fir tree as an alternative to pine timber which is more commonly used in the timber construction industry.

3.2 Strength and Stiffness

The strength and initial stiffness values of the test specimens are investigated by examining the envelope load–displacement curves of the test specimens.

The strength and stiffness of the test specimens were mainly affected by the variables such as aspect ratio, location and size of the openings, timber material and nail spacing. Increasing aspect ratios of the test specimens also significantly increased the strength of the specimens. The aspect ratios of the test specimens were varying between 0.45 and 1.13. The maximum lateral load-resisting capacity of the Specimen 2 with an aspect ratio of 1.13 was 1.7 times larger than that of Specimen 12 with an aspect ratio of 0.68 and 3.2 times larger than that of Specimen 9 with an aspect ratio of 0.45. The maximum lateral load-resisting capacity of the Specimen 3 with an aspect ratio of 1.13 was 3.16 times larger than that of Specimen 11 with an aspect ratio of 0.45. The maximum lateral load-resisting capacity of the Specimen 4 with an aspect ratio of 1.13 was 3.05 times larger than that of Specimen 10 with an aspect ratio of 0.45.

Test specimens 2, 3 and 4 were manufactured using spruce tree, fir tree and pine timbers, respectively, with identical aspect ratios of 1.13. From the comparison of their maximum load-resisting capacities, it was observed that the maximum load-resisting capacity of Specimen 2 (spruce tree timber) was 7% larger than that of Specimens 3 (fir tree timber) and 12% larger than that of Specimen 4 (pine tree timber). Similarly, from the comparison of specimens 9, 10 and 11 with identical properties except their timber types, it was observed that the maximum load-resisting capacity of Specimen 9 (spruce tree timber) was 7% larger than that of Specimens 10 (pine tree timber) and 6% larger than that of Specimen 11 (fir tree timber). These results illustrated that the maximum load-resisting capacities of the test specimens manufactured from spruce tree timber were larger than those of other specimens manufactured from other types of timbers. Also, it should be noted that the ratio between maximum load-resisting capacities of test specimens manufactured from different types of timbers is nearly constant regardless of aspect ratio.

Another variable affecting the performance of the test specimens was the presence of window or door openings. The presence of such openings resulted in reduced lateral load-resisting capacities. From the comparison of test results obtained from specimens with identical aspect ratios but different opening ratios, it was observed that the increasing opening ratio decreased the maximum load-resisting capacity. Specimen 1, with an opening ratio of 2%, Specimen 5, with an opening ratio of 26%, and Specimen 8, with an opening ratio of 30%, have identical aspect ratios and manufactured using spruce tree timber. From the test results, it was observed that the maximum load-resisting capacity of Specimen 1 was 12 and 72% larger than those of Specimens 5 and 8, respectively. From the comparison of results obtained from the tests of specimens having 26% opening ratios, it was observed that Specimen 5 (spruce tree timber) resisted 3 and 11% more loads than Specimen 6 (fir tree timber) and Specimen 7 (pine tree timber), respectively. Specimen 2 (spruce tree timber) without any openings resisted 2.34 times larger load than that of Specimen 8 with the highest opening ratio. These comparative results indicated that the increasing opening ratio significantly decreased the load-resisting capacities of the timber frame panels.

Nail spacing is another effective factor on the variation of load-resisting capacities. Test specimen 12, with an aspect ratio of 0.68, was manufactured using 100 mm nail spacing along the sides of OSB plates and 300 mm nail spacing at the mid regions. Specimen 13 with an aspect ratio of 0.68 was manufactured with 300 mm nail spacing at the sides of the OSB plate and mid regions. From the comparison of Specimens 12 and 13, it was observed that the load-resisting capacity of Specimen 12 was 28% larger than that of Specimen 13. It may be concluded that the increasing nail spacing decreases the load-resisting capacity.

Initial stiffness values were calculated two times for each test specimen by calculating the ratio between the load and displacement values of first loading cycles in both directions and presented in Table 3. The maximum of two

initial stiffness (i.e., the maximum initial stiffness value calculated for both loading directions) is presented as the initial stiffness of the test specimen. From the inspection of initial stiffness values, it was observed that variables considered in the study were significantly effective on the variation of initial stiffness values. As the aspect ratios increased, the initial stiffness values significantly increased. Initial stiffness of Specimen 2 (with an aspect ratio of 1.13) was 7.85 times larger than that of Specimen 9 (with an aspect ratio of 0.45) and 1.03 times larger than that of Specimen 12 (with an aspect ratio of 0.68).

Initial stiffness of Specimen 3 (with an aspect ratio of 1.13) was 15.5 times larger than that of Specimen 11 (with an aspect ratio of 0.45). Initial stiffness of Specimen 4 (with an aspect ratio of 1.13) was 7 times larger than that of Specimen 10 (with an aspect ratio of 0.45). The presence of openings also affected the initial stiffness values of the test specimens. From the test results obtained from the comparison of specimens with identical aspect ratios, it was observed that increasing opening ratios significantly reduced the initial stiffness of the test specimens. Initial stiffness of Specimen 2 (without any opening) was 11% larger than that of Specimen 1 (with an opening ratio of 2%) and 71% larger than that of Specimen 5 (with an opening ratio of 26%). Also, initial stiffness of Specimen 2 (without any opening) was 5.07 times larger than that of Specimen 8 (with an opening ratio of 30%). From the comparison of specimens with openings, it was observed that the increasing opening ratio decreased the initial stiffness values. Specimen 1 (with an opening ratio of 2%) was 1.5 times larger than that of Specimen 5 (with an opening ratio of 26%) and was 4.5 times larger than that of Specimen 8 (with an opening ratio of 30%).

As stated before, another variable considered in the study was the type of the timber used in the construction of test specimens. The initial stiffness values of test specimens constructed using spruce tree, fir tree and pine tree timbers are comparatively presented in this section. From the comparison of test specimens with identical aspect and opening ratios, it was observed that the initial stiffness value of the test Specimen 5 (spruce tree timber) was 1.8 and 1.5 times larger than those of Specimens 6 (fir tree timber) and 7 (pine tree timber), respectively. From the comparison of test specimens with identical aspect ratios and without any openings, it was observed that the initial stiffness value of the test Specimen 9 (spruce tree timber) was twice Specimen 11's (fir tree timber) initial stiffness.

3.3 Displacement Ductility Ratio

Ductility is an important factor on the earthquake resistance of the structure. The displacement ductilities of the test specimens are calculated by dividing the failure displacement to the displacement at the maximum load. The load corresponding to the 85% of the maximum load was assumed to be failure load and the displacement at the failure load was assumed to be the failure displacement. The maximum of the displacement ductilities calculated for back and forth is presented in Table 3.

The aspect ratios, presence of the openings and nail spacings are important factors affecting the displacement ductilities. The increasing aspect ratios increased the displacement ductilities in a small amount. The displacement ductility of the Specimen 2 with an aspect ratio of 1.13 was 40% larger than that of Specimens 9 with an aspect ratio of 0.45 and 36% larger than that of Specimen 12 with an aspect ratio of 0.68.

The presence of door and window openings resulted in a ductile behavior. The increasing opening ratios also increased the level of ductility. The ductility levels of test specimens, constructed from same timber type and with identical aspect ratios and opening ratios, are compared. The displacement ductility of the Specimen 8 (spruce tree timber) with an opening ratio of 30% was 35% larger than that of Specimen 5 with an opening ratio of 26 and 67% larger than that of Specimen 1 with an opening ratio of 2%. From the comparison of test specimens with and without openings, it is observed that the specimens with openings exhibit a more ductile behavior than those of specimens with out openings. The displacement ductility of the Specimen 4 without any opening was 12% smaller than that of Specimen 7 with a large opening.

Also, the effect of timber type on the variation of displacement ductility is considered in this study. The specimens 2 (spruce tree timber), 3 (fir tree timber) and 4 (pine tree timber) have identical properties except the timber type used in the construction of specimens. From the comparison, it is observed that the displacement ductility of the Specimen 2 is the largest and the displacement ductility of the Specimen 3 is the smallest. The displacement ductility of Specimen 2 is 22% larger than that of specimen 2.

From the comparison of test specimens with 26% openings, it is observed that the displacement ductility of Specimen 5 (spruce tree timber) is 36% larger than that of Specimen 6 (fir tree timber) and 5% smaller than that of Specimen 7 (pine tree timber). The presence of openings decreases the strength and stiffness but increases the ductility of the specimens. From the comparison of timber types, the highest ductilities values are observed at the specimens constructed using pine tree timber. An increase in the spacings of nails, used to connect frame elements and OSB plates, also increased the ductility of the specimens. The displacement ductility of specimen 13 with 300 mm nail spacing was 17% larger than that of Specimen 12 with 100 mm nail spacing. Increasing nail spacing

decreases the stiffness but increases the displacement ductility. Specimen-8 is the specimen with largest opening. Accordingly, its stiffness is smaller than other specimens which lead to large deformations in lower level of loading. The small dimensions of panels located between the openings lead to such reduced stiffness and increased deformations. In relation to that, the horizontal displacement ductility of the specimen was high.

3.4 Energy Dissipation Capacity

Energy dissipation capacity is an important factor for the design of earthquake-resistant structures. The energy dissipation capacities of the test specimens are calculated by summing the areas under hysteretic load–displacement relations. The results from experimental study illustrated that the energy dissipation capacity was significantly affected by aspect ratio. The increasing aspect ratio increased the energy dissipation capacities of the test specimens. The energy dissipation capacity of the test specimens 2 with an aspect ratio of 1.13 was 6.22 times larger than that of specimen 9 with an aspect ratio of 0.45 and 3.21 times larger than that of specimen 12 with an aspect ratio of 0.68. The average energy dissipation capacity of test specimens with 1.13 aspect ratio and without any opening was 2.5 and 5.22 times larger than that of specimens with 0.68 and 0.45 aspect ratio and without any opening, respectively.

From the test results, it was observed that the energy dissipation capacities of the test specimens manufactured from different type of timbers with identical aspect ratios did not differ considerably. For example, the energy dissipation capacities of test specimens 9 (spruce tree timber), 10 (pine tree timber) and 11 (fir tree timber) were quite similar. Consequently, it was observed that the type of timber used in the construction of test specimens is not an effective factor on the variation of energy dissipation capacities. From the comparison of specimens (with identical aspect ratios) with and without any openings, it was observed that the energy dissipation capacities of test specimens with openings were smaller than those of their counterparts without any openings. Moreover, it was observed that increasing opening ratio decreases the energy dissipation capacity. The energy dissipation capacity of Specimen 2 (without any openings) is 15064.49 kN-mm while the energy dissipation capacity of Specimen 5 (with 26% opening ratio) is 8106.67 kN-mm and Specimen 8 (with 30% opening ratio) is 6499.88 kN-mm. From these comparisons, it is concluded that the energy dissipation capacity of specimen 2 (without any openings) is twice that of the average energy dissipation capacities of Specimens 5 and 8. From the comparison of test specimens with openings, it is observed that the energy dissipation capacity of the specimen with 2% opening ratio is 9% larger than the average of those specimens with 26% opening ratios and 30% larger than that of specimen with 30% opening ratio. Another factor on the variation of energy dissipation capacities is the nail spacing. The increasing nail spacing results in amplified loads on nail with amplified internal friction. Consequently, the nails permanently deform under loading. The energy arising from loading increment is dissipated by the nails. From the comparison of specimen 12 and specimen 13, the energy dissipation capacity of specimen 12 (with 100 mm nail spacing) was 27% larger than that of specimen 13 (with 300 mm nail spacing):

3.5 Measured Shear Crack

The shear crack width of the test specimens was measured with two electronic deformation measurement devices located diagonally on the panels. The average shear crack widths of the test specimens, calculated by averaging the crack widths of forward and backward loading cycles, are given in Table 4.

From Table 4, it is observed that there is a relation between shear crack widths and aspect ratios. The increasing aspect ratios increased the shear crack widths. From the comparison of specimens without any openings, it was observed that the shear crack width of test Specimen 2 (with an aspect ratio of 1.13) was 5.57 times larger than that of Specimen 9 (with an aspect ratio of 0.45) and 1.13 times larger than that of Specimen 13 (with an aspect ratio of 0.68). The shear crack width of test Specimen 3 (with an aspect ratio of 1.13) was 15.21 times larger than that of Specimen 11 (with an aspect ratio of 0.45).

The opening ratio is another important factor on the variation of shear crack widths. The shear crack widths measured from specimens with openings were larger than those of specimens without any openings. The shear crack width of specimen 2 without any opening was 61 and 43% smaller than those of specimens 5 and 8, respectively. The presence of openings resulted in stress concentrations on the corners of openings and shear cracks related with those stress concentrations caused the enlargement of the measured crack widths.

4 Comparison of Experimental and Eurocode Regulations

The horizontal load-carrying capacities of test specimens obtained by two different methods, proposed by the Eurocode 5 regulations, were compared with the experimental capacity values and the accuracies of analytical methods were considered. The analytical capacity values of the specimens were calculated with the Eurocode 5

Table 4 Shear crack width measurement of specimens

Spec. no	Shear crack width (mm)					
	Left		Right		Average	
	forward cycles	Backward cycles	forward cycles	Backward cycles	forward cycles	Backward cycles
1	4.80	4.97	3.64	8.01	4.22	6.49
2	8.02	8.84	5.00	14.12	6.51	11.48
3	18.60	21.91	20.85	20.39	19.73	21.15
4	14.95	18.68	14.91	19.82	14.93	19.25
5	25.10	22.35	20.73	24.33	22.92	23.34
6	27.17	8.24	13.43	27.44	20.30	17.84
7	20.48	26.58	22.47	25.67	21.48	26.13
8	24.73	4.88	5.54	28.06	15.14	16.47
9	1.24	1.99	1.24	2.13	1.24	2.06
10	2.09	0.21	0.76	1.68	1.43	0.95
11	1.67	1.10	1.11	1.51	1.39	1.31
12	10.17	12.66	11.97	13.72	11.07	13.19
13	8.29	9.01	8.18	10.90	8.24	9.96

regulation, which is used for timber structures in the European countries. The analytical capacity values were compared with the experimental resistance values. According to the computational Eurocode 5 model, the shear walls can be regarded separately, for design purposes, as vertical cantilever beams with horizontal force acting at the top.

In the final version of Eurocode 5 (2004), two simplified computational methods are given to determine the load-carrying capacity of wall diaphragms. The first simplified analysis—Method A—is identical to the ''Lower bound plastic method'', presented by Källsner and Lam, 1995 [38]. The method defines the shear resistance of the wall ($F_{v,\mathrm{Rd}}$) as the sum of the shear resistance of all mechanical fasteners ($F_{f,\mathrm{Rd}}$) along the loaded edges in the form of where $F_{f,\mathrm{Rd}}$ is the lateral design capacity per fastener; b is wall panel width; and s is the fastener spacing (Eqs. 1, 2).

$$F_{v,\mathrm{Rd}} = \sum F_{f,\mathrm{Rd}} \cdot \frac{b}{s} \cdot c \tag{1}$$

$$c \begin{cases} 1 & \text{for } b \geq b_o \\ \dfrac{b}{b_o} & \text{for } b \leq b_o \end{cases} \quad \text{where } b_o = h/2 \tag{2}$$

This is only an approximated and simplified definition, which can be applicable to wood-based panels where the tensile strength is relatively high and the specimens tend to fail because of fastener yielding. In this method, wall panels, which contain a door or window opening, should not be considered to contribute to the rocking load-carrying capacity. The second simplified analysis—method B—is applicable to walls constructed from the sheets of wood-based panel products only fastened to a timber frame. The fastening of the sheets to the timber frame should be either by nail or by screws and the fasteners should be equally spaced around the perimeter of the sheet. Method B is practically a modified version of method A. According to method A, the sheathing material factor, fastener spacing factor, vertical load factor and the dimension factor for the panel are included in the design procedure (Eqs. 3, 4). Using this method where an opening is formed in a panel, the lengths of panel on each side of the opening should be considered as separate panels.

$$F_{v,\mathrm{Rd}} = \sum F_{f,\mathrm{Rd}} \cdot \frac{b}{s_0} \cdot k_d \cdot k_{iq} \cdot k_s \cdot k_n \tag{3}$$

$$\text{where } s_0 = \frac{9700 \cdot d}{\rho_k} \tag{4}$$

The results of the experimental and analytical ultimate strength values of the specimens calculated by using method-A and method-B included in the Eurocode 5 regulations are given in Table 5. Specimens 5–7 have multiple openings with large dimensions and their experimental analytical (i.e., methods A and B in Eurocode 5) capacities are significantly different. Such differences indicated that the methods A and B in Eurocode 5 are not accurate in determining the load-resisting capacities of panels with multiple and irregularly located openings. Such an inaccuracy may be attributed to the difference of load-resisting mechanisms for specimens with multiple large openings. In contrary to that the analytical methods (i.e., using methods A and B in Eurocode 5) lead more accurate results for the

Table 5 Comparison of experimental and Eurocode 5 regulation results

Spec. no	Ultimate load capacity (kN)			Experimental/Eurocode-5 ratio	
	Experimental	Eurocode-5			
		Method A	Method B	Method A	Method B
1	44.99	52.93	48.77	0.85	0.92
2	61.26	76.56	96.58	0.80	0.63
3	57.11	76.56	95.88	0.75	0.60
4	54.24	76.56	101.44	0.71	0.53
5	39.83	15.38	24.03	2.59	1.66
6	38.49	15.38	23.85	2.50	1.61
7	35.81	15.38	25.24	2.33	1.42
8	26.14	15.08	47.35	1.73	0.55
9	19.16	30.48	18.03	0.63	1.06
10	17.78	30.48	19.21	0.58	0.93
11	18.03	30.48	18.16	0.59	0.99
12	35.32	47.67	39.75	0.74	0.89
13	27.53	15.89	16.97	1.73	1.62

case of specimens with one opening or for the case of solid specimen without any opening.

In method A of Eurocode 5, panel parts located above and below the opening do not contribute to the load-resisting capacity of the panel. Due to the opening (522 mm width) of Specimen 1, the width of the panels (3000 mm) of Specimens 2 and 3 is reduced. In relation to the presence of opening, the capacity of Specimen 1 was calculated by adding the capacities of two panel parts (i.e., with 1800 and 600 mm widths). Accordingly, the capacity of Specimen 1, divided by the opening, is smaller than those of Specimens 2 and 3.

5 Numerical Analysis

5.1 Finite Element Model

The numerical analysis is based on the experimental research previously performed on the timber-framed shear wall elements coated with OSB boards. The wall specimens were modeled and analyzed using the commercial FEM computer software ANSYS ver. 14. Timber-framed shear wall specimens consist of several materials such as wood, OSB sheathing panel, mechanical fasteners (nail, screw). A wood-framed shear wall was modeled with beam, shell, and spring elements representing frame members, sheathing panels, and fasteners connecting the sheathing panels to the frame. Spruce tree, Fir tree and Pine tree exhibited nonlinear behavior in tension and compression. OSB sheathing panels exhibited linear behavior in tension and nonlinear behavior in compression. In the finite element modeling of timber wall panels, timber frame elements and OSB plate covering panels were modeled as orthotropic elasto-plastic nonlinear materials. The mechanical fasteners between the timber frame and the sheathing boards (i.e., nails) were modeled according to the two values of slip modulus, serviceability limit state (K_{ser}-SLS) and ultimate limit state (K_u-ULS) [5]. The axial rigidity of nails, used between frame and OSB plates, was calculated by shear modulus from EuroCode 5 [29] (Eqs. 5–7).

$$K_{\text{ser}} = \frac{\rho_m^{1.5} * d^{0.8}}{30} \tag{5}$$

$$\rho_m = \sqrt{\rho_{m,1} * \rho_{m,2}} \tag{6}$$

$$K_u = \frac{2}{3} * K_{\text{ser}} \tag{7}$$

The use of proper elements with a suitable number is vital to obtain accurate results in finite element analyses. To determine the finite element mesh size, a preliminary study was performed and the optimum mesh distribution was determined. The dimensions of the finite elements were determined as 40 mm. To prevent the sliding and rotation of timber-framed panels under reverse cyclic loading, the connection of panels to the ground was provided by steel connection elements. In the finite element models, the connection elements were modeled by attaining fixed support conditions to the nodes. Furthermore, the out-of-plane behavior of OSB plates was prevented by attaining rotation fixities in the x, y and z directions. To impose the loading conditions, a steel part with a length of loading arm was modeled. Multi-step analyses were conducted with the force (F) increments of 5 kN until the ultimate capacity of the structure was reached.

5.2 Verification of Numerical Results

In scope of the study finite element analyses of 13 test specimens, constructed using spruce, fir, pine tree timbers were conducted. In the finite element analyses, static pushover analyses were conducted to compare the experimental envelop curves with the finite element analyses results. Numerical results were verified by comparing load–deflection relationships obtained from cyclic loading test results (Fig. 7). Figure 7 illustrates the good agreement on the lateral load–displacement relationships of experimental and numerical studies. Observed damage in the experimental study was compared with the stress distributions obtained from finite element analyses. The stress distributions in the OSB sheathing panels were taken from the last loading step in the finite element analyses (Fig. 8). From Fig. 8, it was observed that the stress was concentrated at the lower anchoraged regions and at the sides of door and window openings. Such stress concentrations cause damage in the panel walls. Consequently, it may be said that the presence of openings decreases the lateral load-resisting capacity and stiffness of the test specimens. From the comparison, it was observed that the damages observed in the experimental study were in good agreement with the stress concentrations in the finite element analyses. The damage at the lower anchoraged regions and at the sides of door and window openings is given in Fig. 6. Failure modes included a combination of nail pull-through sheathing panels, tear in the OSB panel, sheathing panel edge tear-out and nail heads embedding into panels.

5.3 Comparison of Experimental and Numerical Results

The experimental and numerical results in terms of ultimate loading capacity and corresponding displacement are given in Table 6. From Table 6, it is observed that the results obtained from experimental and numerical study are in good agreement. The difference between the experimental and numerical results in terms of maximum loads and corresponding displacements are 8% and 5%, respectively. It is believed that one of the reasons of the difference between the experimental and numerical results is the handling of boundary conditions. In the finite element study, the boundary conditions were simulated as perfectly rigid without any fabrication errors. On the other hand, in the experimental case, it is very hard to provide such perfect boundary conditions. Finite element modeling of the imperfections in the boundary conditions is not an easy procedure. Another reason for the difference in the experimental and numerical study is the nails used in the connection points of panel and frame elements. The

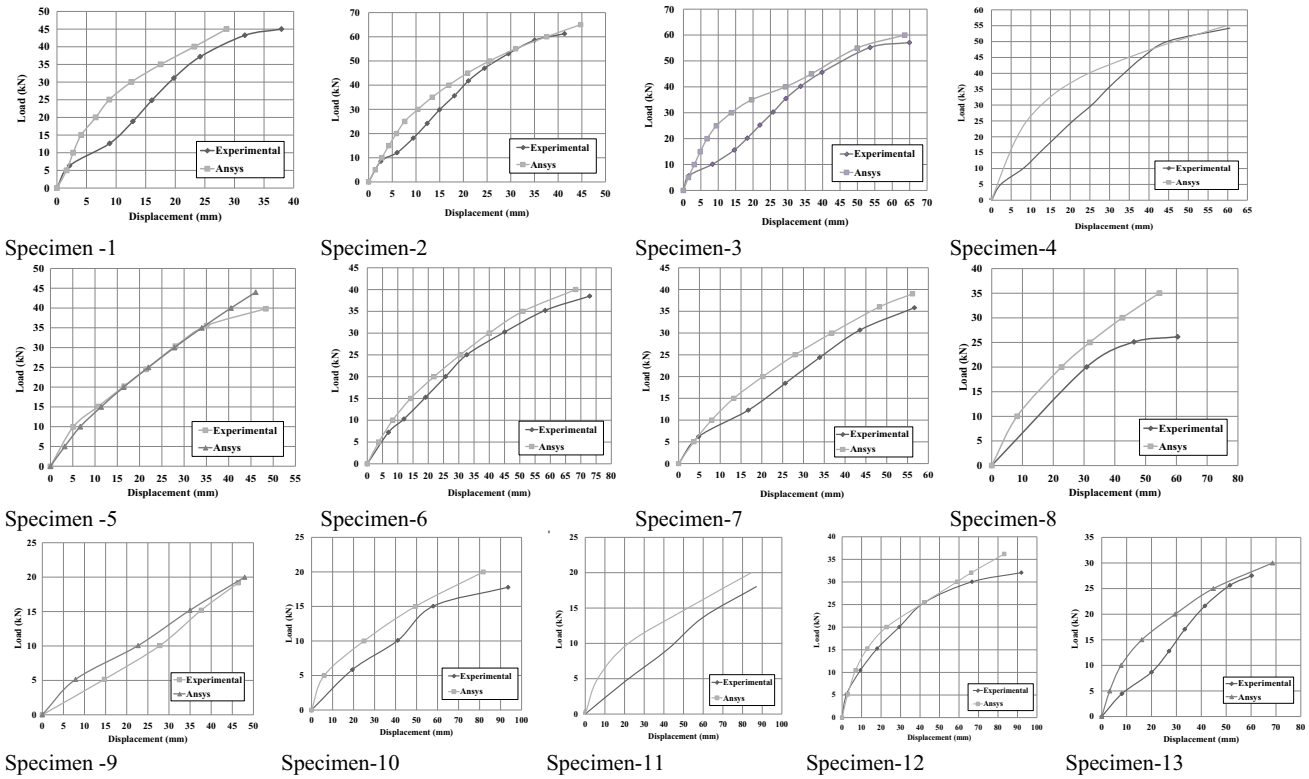

Fig. 7 Comparison between numerical and experimental load versus displacement curves under loading

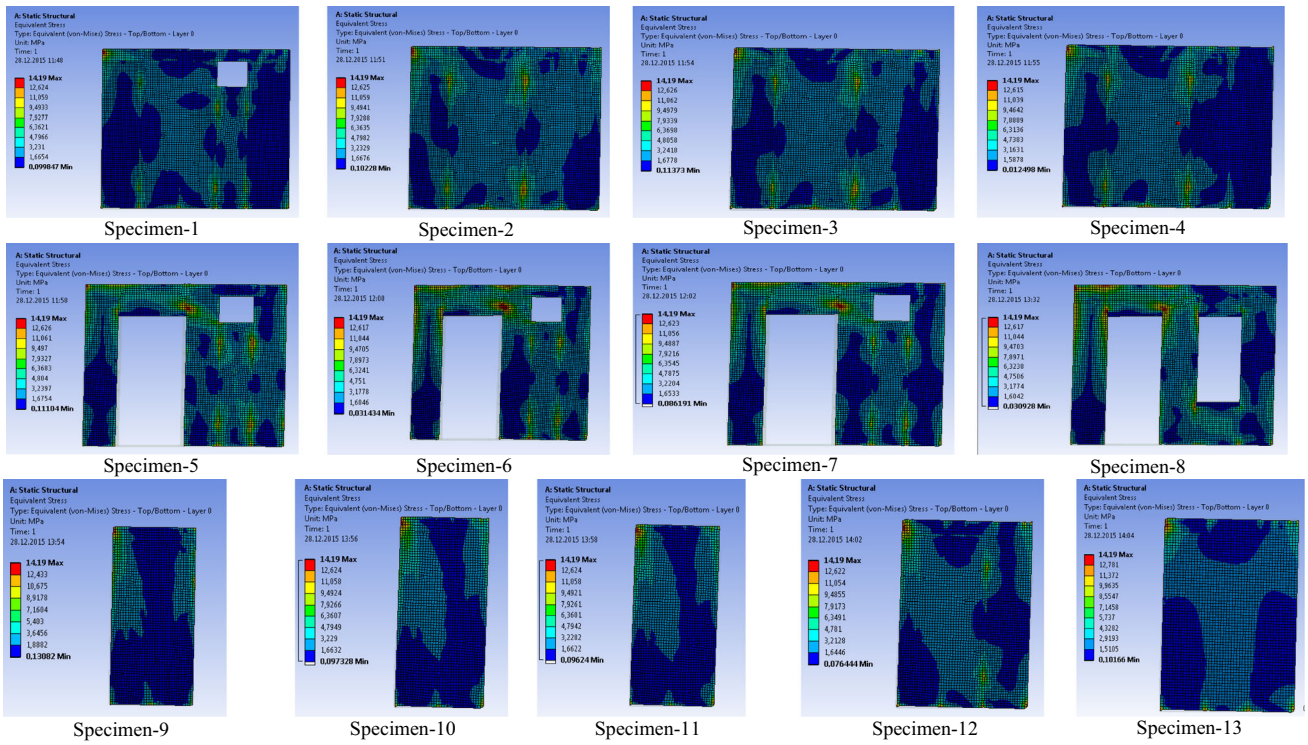

Fig. 8 The stress distribution in the OSB sheathing panels at ultimate load

Table 6 Comparison of experimental and numerical results

Spec. no	Ultimate load (kN)			Displacement at the ultimate load (mm)		
	Experimental	FEM	Exp./FEM ratio	Experimental	FEM	Exp./FEM ratio
1	44.98	45.00	1.00	37.94	28.65	1.32
2	61.26	65.00	0.94	41.36	44.74	0.92
3	57.11	60.00	0.95	64.97	63.61	1.02
4	54.24	55.00	0.99	60.51	59.68	1.01
5	39.83	44.00	0.91	48.37	46.09	1.05
6	38.49	40.00	0.96	72.90	68.36	1.07
7	35.81	40.00	0.90	56.65	56.17	1.01
8	26.14	35.00	0.75	60.38	54.43	1.11
9	19.17	20.00	0.96	46.40	47.93	0.97
10	17.78	20.00	0.89	93.59	81.80	1.14
11	18.03	20.00	0.90	87.03	84.50	1.03
12	32.06	36.20	0.89	92.02	83.25	1.11
13	27.53	30.00	0.92	60.25	68.63	0.88

deformation capabilities of these nails were calculated according to Eurocode 5 regulations. The nails used in these connections were modeled as spring elements characterized with Eurocode 5 regulations. It is believed that such a modeling approach is not capable of fully representing the plastic deformation and actual nonlinear behavior. In the actual behavior, the nail beds deviate from their initial position due to the accumulation of damage. However, in the modeling approach, a spring is used in each nail region.

From the experiments, it is observed that the damage and cracks on panel walls were concentrated in two regions. The first region is the corners of the openings on panels and the second region is the vicinity of anchorage plates used to support the timber panel walls. Concentration of cracks on test specimens, out-of-plane buckling of

OSB plates and cracks in the regions of junction points are also observed from the damage states given in Fig. 6. From Fig. 8, it is observed that the peak points of stress distributions, obtained from numerical analyses, generally coincide with the damaged regions (i.e., anchorage points of panel walls, corners of openings and junction points of OSB plates) given in Fig. 6. In light of the above discussions, it is concluded that the damage observations from the experimental and numerical studies agree well with each other.

6 Conclusions

In scope of the study, behavior of the timber-framed shear walls having openings with variable dimensions and locations subjected to reverse cyclic loading is experimentally and numerically investigated. Furthermore, in scope of the study, the ultimate strength values of timber-framed panels were calculated with two different methods proposed by the Eurocode 5 regulations and compared with experimental results. The main variables considered in the study are the aspect ratios of timber-framed panel walls, dimensions and locations of the openings on the panel walls, material of the timber frames and spacings of the nails used in the panel connections.

The main conclusions deduced from study are listed below:

- Decreasing aspect ratio of the test specimens resulted in bending dominated behavior and a large portion of observed displacements was observed as bending displacements.
- The panels without any openings have larger lateral stiffness and load-resisting capacity relative to the panels with openings.
- The performance of specimens with identical aspect ratios and properties was compared in terms of the type of material. From the comparison, it is observed that the highest performance was displayed by Spruce tree.
- In the study, the effect of nail spacings on the performance was considered experimentally. From the experimental results, it is observed that the strength of the panels decreased with increasing nail spacing.
- In the method A of Eurocode 5, the wall elements with door and window openings do not contribute to the lateral load-resisting capacity. In Method B, separate parts located at the sides of the openings are considered as discrete panels and contribute to the lateral load-resisting capacity. In relation to that, the lateral load-resisting capacities calculated using method B are larger than those obtained using method A.

In the second part of the study, finite element analyses of the test specimens were conducted. A wood-framed shear wall was modeled with beam, shell, and spring elements representing frame members, sheathing panels, and fasteners connecting the sheathing panels to the frame. Such a modeling strategy resulted in a simplified model with decreased analyses times. In the finite element modeling of timber wall panels, timber frame elements and OSP plate covering panels were modeled as orthotropic elasto-plastic nonlinear materials. The numerical and experimental results were compared in this study. The conclusions deduced from the numerical analyses were summarized below:

- A good agreement was observed from the comparison of numerical and experimental results.
- The observed damage in the experimental study is compared with the stress distributions obtained from finite element analyses. It was observed that the stress was concentrated at the lower anchoraged regions and at the sides of door and window openings. From the comparison, it was observed that the damages observed in the experimental study were in good agreement with the stress concentrations in the finite element analyses.

Acknowledgements This study is the No. 01332STZ.2012-1 San-Tez project supported by the Ministry of Science, Industry and Technology. The authors would like to express their gratitude to the Ministry and to the Şanver Furniture, Decoration, Construction Forest Products Corporation for their support of the Project.

References

1. Silih EK, Premrov M (2010) Analysis of timber-framed wall elements with openings. Constr Build Mater 24:1656–1663
2. Thelandersson S, Larsen HJ (2003) Timber engineering. Wiley, Chichester
3. Premrov M, Kuhta M (2010) Experimental analysis on behaviour of timber-framed walls with different types of sheathing boards. Construction materials and engineering. Nova Science Publishers, Inc, New York
4. Pintaric K, Premrov M (2013) Mathematical modelling of timber-framed walls using fictive diagonal elements. Appl Math Model 37:8051–8059
5. Šilih EK, Premrov M, Šilih S (2012) Numerical analysis of timber-framed wall elements coated with single fibre-plaster boards. Eng Struct 41:118–125
6. Premrov M, Kuhta M (2008) Influence of fasteners disposition on behavior of timber-frame walls with single fibre-plaster sheathing boards. Constr Build Mater 23:2688–2693
7. Dobrila P, Premrov M (2003) Reinforcing methods for composite timber frame fibreboard wall panels. Eng Struct 25(11):1369–1376
8. Premrov M, Dobrila P, Bedenik BS (2004) Analysis of timber-framed walls coated with CFRP strips strengthened fibre-plaster boards. Int J Solid Struct 41(24/25):7035–7048
9. Premrov M, Dobrila P, Bedenik BS (2004) Approximate analytical solutions for diagonal reinforced timber-framed walls with fibre-plaster coating material. Constr Build Mater 18(10):727–735

10. Premrov M, Kuhta M (2009) Influence of fasteners disposition on behavior of timber-framed walls with single fibre-plaster sheathing boards. Constr Build Mater 23(7):2688–2693
11. Premrov M, Dobrila P (2012) Numerical analysis of sheathing boards influence on racking resistance of timber-frame walls. Adv Eng Softw 45(1):21–27
12. Šilih EK, Premrov M (2012) Influence of openings on horizontal load-carrying capacity of timber-frame wall element with fibre-plaster sheathing boards. Adv Eng Softw 43(1):19–26
13. Anıl Ö, Altın S (2007) An experimental study on reinforced concrete partially infilled frames. Eng Struct 29:449–460
14. Park J (2016) Investigation of the geometric variation effect on seismic performance of low-rise unreinforced masonry structures through fragility analysis. Int J Civ Eng. doi:10.1007/s40999-016-0070-x
15. Richard N, Yasumura M, Davenne L (2003) Prediction of seismic behavior of wood framed shear walls with openings by pseudo-dynamic test and FE model. J Wood Sci 49:145–151
16. Yasumura M, Sugiyama H (1984) Shear properties of plywood-sheathed wall panels with opening. Trans Archit Inst Jpn 338:88–98
17. Kuhta M, Premrov M (2008) Influence of fasteners disposition on behavior of timber-frame walls with double fibre-plaster coating boards. Am J ApplSci 5(1):1–6
18. Meghlat EM, Oudjene M, Ait-Aider H, Batoz JL (2013) A new approach to model nailed and screwed timber joints using the finite element method. Constr Build Mater 41:263–269
19. Baylor G, Harte AM (2013) Finite element modelling of castellated timber I-joists. Constr Build Mater 47:680–688
20. Boudaud C, Humbert J, Baroth J, Hameury S, Daudeville L (2014) Joints and wood shear walls modelling II: experimental tests and FE models under seismic loading. Eng Struct 101:743–749
21. Loo WY, Quennevillea P, Chouw N (2012) A numerical approach for simulating the behaviour of timber shear walls. Struct Eng Mech 42(3):383–407
22. Blasetti AS, Hoffman R, Dinehart D (2008) Simplified hysteresis finite-element model for wood and viscoelastic polymer connections for the dynamic analysis of shear walls. J Struct Eng 134(1):77–86
23. Gupta AK, Kuo GP (1987) Modeling of a wood-framed house. J Struct Eng ASCE 113(2):260–278
24. Ayoub A (2007) Seismic analysis of wood building structures. Eng Struct 27(2):213–223
25. Guan ZW, Zhu EC (2009) Finite element modelling of anisotropic elasto-plastic timber composite beams with openings. Structures 31:394–403
26. Polensek A (1976) Finite-element analysis of wood-stud walls. J Struct Div ASCE 102(7):1317–1335
27. Richard N, Daudeville L, Prion H, Lam F (2002) Timber shear walls with large openings: experimental and numerical prediction of the structural behavior. Can J Civ Eng 29:713–724
28. Pang W, Rosowsky D (2010) Beam-spring model for timber diaphragm and shear walls. Struct Build 163(SB4):227–244
29. EN 1995-1-1 (2010): Eurocode 5: design of timber structures—Part 1–1: general—common rules and rules for buildings; German version EN 1995-1- 1:2004+AC:2006+A1:2008. European Committee for Standardization, Brussels
30. TS 2472 (1976) Wood—determination of density for physical and mechanical tests. TSE, Ankara
31. TS 2478 (1976) Wood-determination of modulus of elasticity in static bending. TSE, Ankara
32. TS 2475 (1976) Wood-determination of ultimate tensile stress parallel to grain. TSE, Ankara
33. TS 2595 (1977) Wood-determination of ultimate stress in compression parallel to grain. TSE, Ankara
34. TS EN 323 (1999) Wood-based panels-determination of density. TSE, Ankara
35. TS EN 3 (1999) Wood-based panels-determination of modulus of elasticity in bending and of bending strength. TSE, Ankara
36. ASTM D3500-14 (2014) Standard test methods for structural panels in tension. ASTM International, West Conshohocken, PA
37. ASTM D3501-05a (2011) Standard test methods for wood-based structural panels in compression. ASTM International, West Conshohocken, PA
38. Källsner B, Lam F (1995) Diaphragms and shear walls. Holzbauwerke: Grundlagen, Entwicklungen, Ergänzungennach Eurocode 5, step 3, Fachverlag Holz, Düsseldorf, p 15/1–19